ELSEVIER
Science Press
Available online at www.sciencedirect.com
ScienceDirect
Trans. Nonferrous Met. Soc. China 35(2025) 2777−2789
Transactions of Nonferrous Metals Society of China
www.tnmsc.cn

Preparation of AlF_3 from waste aluminum electrolyte via leaching, electrolysis, and roasting

Xiao-jun LV, Xuan TAN, Ze-xun HAN, Li-qiong LUO, Yong-cong WU

School of Metallurgy and Environment, Central South University, Changsha 410083, China

Received 13 December 2023; accepted 20 May 2024

Abstract: High-purity AlF_3 was prepared by the combined process of leaching the raw material of waste aluminum electrolytes with aluminum chloride, electrolyzing the leaching solution, and then mixing with ammonium hydrogen fluoride for roasting. Under the optimal leaching conditions of a fluorine to aluminum molar ratio of 2.0, a liquid-to-solid ratio of 12, a temperature of 90 °C, and time of 4 h, the fluorine leaching rate can reach 99.15%. Under the action of electrolysis, the H^+ is reduced to H_2 in the cathode, while the remaining OH^- combines with AlF^{2+} and AlF_2^+ to precipitate aluminium hydroxyfluoride hydrate. The results show that electrolysis is beneficial to reduce the impurity content of aluminium hydroxyfluoride hydrate. When the current density is 0.2 A/cm^2, the temperature is 90 °C, the stirring speed is 200 r/min, and the electrolysis endpoint pH is 3.0, the total content of Na, K and Ca impurities in the precipitation is only 0.64 wt.%. Moreover, the hydrolysis can be inhibited effectively by adding ammonium hydrogen fluoride in the mixed-roasting process. When the mass ratio of aluminium hydroxyfluoride hydrate to ammonium hydrogen fluoride is 2:1, the purity of the AlF_3 product is even 99.51 wt.%. Conducively, the high-purity AlF_3 can be returned to the aluminum electrolysis industry or used as a reagent.

Key words: waste aluminum electrolyte; aluminum chloride solution; electrolysis; aluminium hydroxyfluoride hydrate; ammonium hydrogen fluoride; anhydrous aluminum fluoride

---

1 Introduction

In the production process of primary aluminum, it is necessary to add 15−20 kg of aluminum fluoride to the electrolyte for every ton of primary aluminum to maintain a stable cryolite ratio [1−3]. Based on the principle of conservation of mass, the addition of fluorine salts will produce the equivalent number of electrolytes, increasing the electrolyte level in the electrolytic cell [4−9]. Therefore, surplus electrolytes must be scooped periodically for storage, which can also be useful to start up new electrolysis cells or overhaul ones later [10−13]. What should also be noticed is that some of the electrolytes were entrained in carbon slags or overhaul slags [14,15]. With the existing electrolytic aluminum production capacity in China close to saturation, the construction of new domestic aluminum electrolytic cells has significantly decreased, which is bound to lead to a substantial accumulation of electrolytes [16]. If effective measures are not taken, the spent aluminum electrolytes, containing a high concentration of soluble fluorine, will pose significant security risks to the ecological environment [17−21]. Consequently, it is an important and pressing issue for the whole aluminum industry to realize the safe disposal and efficient recycling of fluorine-containing secondary resources [22].

The primary constituents of the waste aluminum electrolyte include Na_3AlF_6, LiF, KF, AlF_3, CaF_2, Al_2O_3 and C. Its phase composition is intricate,

---

Corresponding author: Ze-xun HAN, Tel: +86-17375896074, E-mail: hanzexun@csu.edu.cn
https://doi.org/10.1016/S1003-6326(25)66847-6

making the extraction of valuable elements challenging. Currently, both domestic and international research focuses on recovering fluorine from waste aluminum electrolytes by converting it into various forms of fluorine compounds such as aluminum hydroxyfluoride hydrate, cryolite and calcium fluoride [23−28]. The aluminium hydroxyfluoride hydrate, serving as an intermediate product, is primarily obtained by using lye to adjust the pH of the leaching solution. The aluminum fluoride is obtained by directly roasting aluminium hydroxyfluoride hydrate or mixing with hydrofluoric acid to roast [29−31].

BUSH and GAYDOSIK [32] utilized sodium hydroxide to neutralize acidic solutions that contain Na, Al and F, and adjusted the pH to 2.0−3.0 to precipitate aluminium hydroxyfluoride hydrate, upon undergoing roasting which can yield aluminum fluoride. Their research revealed that the content of Na and S in aluminium hydroxyfluoride hydrate accounted for 2.06% and 1.73%, whereas the roasted products contained 0.83% Na and 0.69% S. Furthermore, XRD analysis demonstrated that the roasted products not only contained aluminum fluoride but also exhibited a small peak corresponding to the oxide phase of sodium and aluminum. WU et al [33] utilized a combination of diluted sulfuric acid and aluminum salt to leach the waste anode cover material of aluminum electrolysis. After that, a sodium hydroxide solution was employed to adjust the pH of the leaching solution to precipitate aluminium hydroxyfluoride hydrate, which was later mixed with hydrofluoric acid for roasting to finally obtain aluminum fluoride. In their study, the XRD analysis of both the precipitation and the final product revealed a few miscellaneous peaks. Furthermore, the chemical composition of the final product showed that the Na content was 1.25% and the SO_4^{2-} content was 10.3%. LISBONA and STEEL [34] employed a two-stage leaching process to recover fluorine from spent pot-lining. The process involved water washing to remove NaF from the raw materials, followed by leaching the dried filter cake with aluminum nitrate solution to obtain the leaching solution. After that, the pH of the solution was adjusted by adding sodium hydroxide to obtain aluminium hydroxyfluoride hydrate. Subsequently, aluminum fluoride was obtained by roasting at high temperature. In their study, aluminium hydroxy- fluoride hydrate was precipitated under the optimal conditions of 70 °C and pH 4.5, in which the Na content was 2.52% by EDS analysis. The XRD analysis revealed the appearance of cryolite impurities in the sediment with the increase in pH. The content of Na in aluminum fluoride obtained by roasting at 485 °C was 2.45%. According to the analysis [34], the aluminium hydroxyfluoride hydrate would decompose into aluminum fluoride, alumina, and hydrogen fluoride during direct roasting, and the hydrolysis would be promoted as the temperature increased. Recently, HAN et al [24] proposed a process of combining NaF roasting with aluminum sulfate leaching to extract lithium from waste aluminum electrolytes. Notably, the step of adjusting the pH of the leaching solution to 6.6 by adding NaOH solution resulted in 99.26% recovery of Al and 97.21% recovery of F. However, the Na content of the aluminium hydroxyfluoride hydrate precipitation was as high as 11.49%, and the XRD pattern showed that the sodium existed in the form of cryolite.

To sum up, Na or K introduced by using lye to adjust pH in the existing process promotes the precipitation of cryolite impurities, which reduces the purity of aluminium hydroxyfluoride hydrate, and therefore further diminishes the effectiveness of aluminum fluoride products in adjusting the cryolite ratio of aluminum electrolytes. Moreover, the aluminium hydroxyfluoride hydrate will result in hydrolysis by direct roasting and reduce the purity of the aluminum fluoride, while the process of hydrofluoric acid roasting has high equipment requirements and is complicated.

In this study, the aluminum chloride solution was used as a leaching agent to leach waste aluminum electrolytes, and then the leaching solution was electrolyzed to precipitate aluminium hydroxyfluoride hydrate. Finally, the precipitation mixed with ammonium hydrogen difluoride was roasted to obtain anhydrous aluminum fluoride. This process provided a new way of preparing anhydrous aluminum fluoride from fluorine-containing materials.

2 Experimental

2.1 Materials

The waste aluminum electrolyte used in the experiment was provided by an electrolytic aluminum plant in China, and the main components are listed in Table 1.

The XRD patterns of the waste aluminum electrolyte are shown in Fig. 1. The composition of raw materials is complex, which is mainly composed of Na_3AlF_6, NaF, AlF_3, and CaF_2, and also contains a small amount of lithium sodium composite cryolite and carbon. By XRF and ICP detection, the content (mass fraction) of each compound in the raw material was calculated to be 3.59% potassium fluoride, 5.25% lithium fluoride, 4.03% calcium fluoride, 0.45% magnesium fluoride, and 2.65% alumina, with the remaining content being cryolite of the molecular ratio of 2.3.

Table 1 Main components of waste aluminum electrolyte (wt.%)

F	Al	Na	K	O	Mg	Ca	Li
49.78	13.81	27.72	2.65	1.73	0.20	2.54	1.57

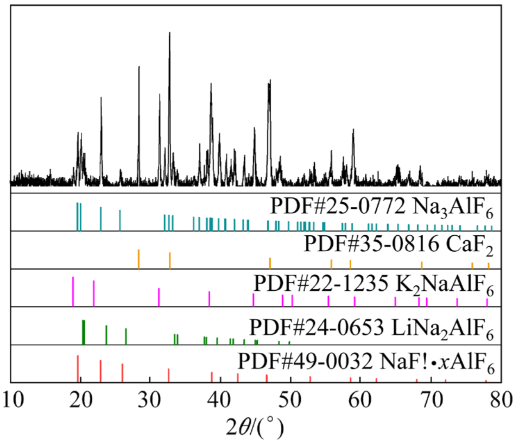

Fig. 1 XRD patterns of waste aluminum electrolyte

2.2 Technological processes and equipment

In this research, the process flowchart of preparing high-purity aluminum fluoride by recycling waste aluminum electrolyte is shown in Fig. 2, including three main processes: leaching, electrolysis, and roasting. All reagents used in the experiment are analytically pure.

The electrolysis device used in the experiment is shown in Fig. 3. The electrolysis cell body was constructed with organic glass, and the ruthenium−iridium−coated titanium plate was used as the cathode and anode. The electrolysis cell is divided into a cathode chamber and an anode chamber by a cation-exchange membrane.

2.3 Methods

2.3.1 Test scheme

(1) Leaching test

The waste aluminum electrolyte was broken and sifted into less than 150 μm for future use. The reagents used in the experiment are all of analytical purity, and water is the first-grade purity.

Aluminum chloride solution was used as the leaching agent. The optimal experimental conditions for leaching waste aluminum electrolyte were investigated by setting single-factor parameters, such as the molar ratio of fluorine to aluminum (F/Al) of 1.6−2.8, the ratio of liquid to solid (L/S) of 8−12, leaching temperature of 60−95 °C, and leaching time of 2−12 h.

Based on the XRF test results of raw materials, the final F/Al of the leaching solution was adjusted by adding aluminum chloride. The amount of aluminum chloride was calculated by

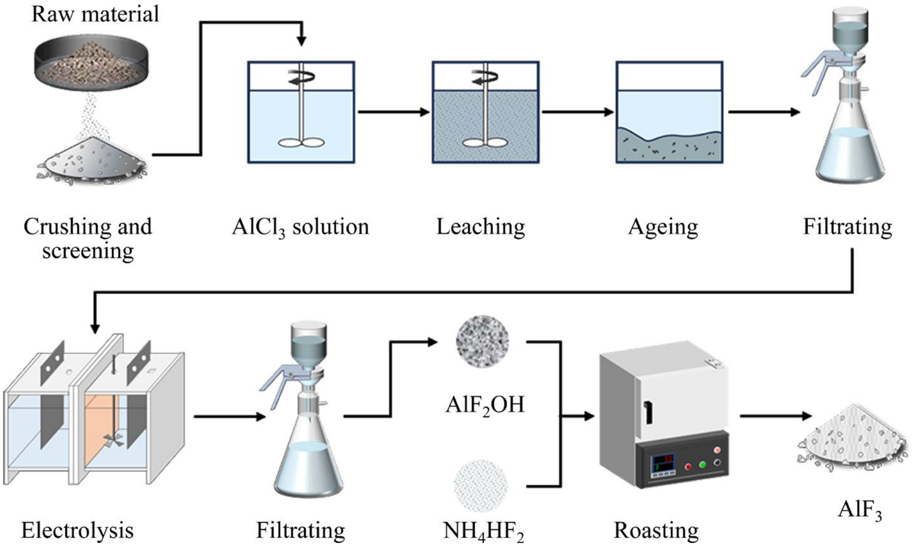

Fig. 2 Process flowchart for preparation of high-purity aluminum fluoride

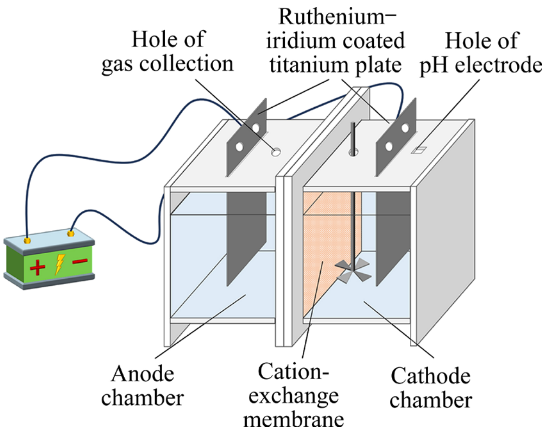

Fig. 3 Schematic diagram of electrolysis device

$$m=\frac{m_{\mathrm{w}}\left(Y-K\right)M}{211.39K} \tag{1}$$

where K is the control target of F/Al ratio, M is the relative molecular mass of the leaching agent $AlCl_3$, m is the mass of the leaching agent (g), m_{w} is the mass of waste aluminum electrolyte (g), Y is the F/Al ratio of waste aluminum electrolyte, and 211.39 is the coefficient of aluminum salt supplementation based on the composition of waste aluminum electrolyte.

(2) Electrolysis test

The leaching solution obtained in Step (1) was electrolyzed. During electrolysis, the chlorine gases produced in the anode chamber were exported through a collector hole, which is sealed with a double-hold rubber plug, and absorbed by the NaOH solution. The pH of the electrolytic solution is monitored in real-time using a high-temperature resistant pH electrode. After the electrolysis is completed, the slurry is filtered to separate the solid and liquid. The aluminium hydroxyfluoride hydrate precipitation was washed and dried, and the filtrate can be circulated for leaching.

The basic principle of the preparation of high-purity aluminium hydroxyfluoride hydrate by an electrolytic method is the redox reaction that occurs on the contact surface of the electronic conductor (electrode) and the ionic conductor (leaching solution). The anode and cathode chemical reaction equations are as follows:

Anode: $2Cl^{-}-2e\rightarrow Cl_2\uparrow$ (2)

Cathode: $2H_2O+2e\rightarrow 2H_2\uparrow+2OH^{-}$ (3)

$$\mathrm{AlF}_i^{3-i}+(3-i)\mathrm{OH}^-\rightarrow \mathrm{AlF}_i(\mathrm{OH})_{3-i}\downarrow\ \ (1\le i\le 3) \tag{4}$$

The electrolytic process diagram is shown in Fig. 4.

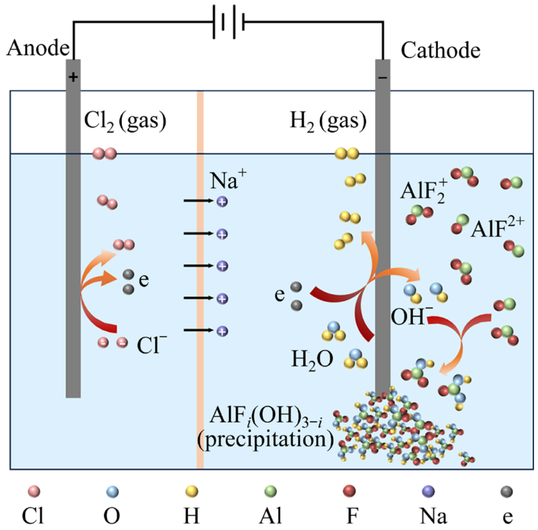

Fig. 4 Diagram of electrolysis process

Under the action of electrolysis, hydrogen bubbles up from the cathode plate. The hydroxide ion (OH^{-}) in the cathode region produces and combines with AlF^{2+} and AlF_2^{+} ions in the solution to form aluminium hydroxyfluoride hydrate precipitates. Compared with the traditional method of adding lye, electrolysis can effectively avoid the precipitation of cryolite impurities due to the increasing local alkali concentration. After the electrolysis is completed, the solutions of the cathode chamber and the anode chamber can be mixed and then electrolyzed in succession by supplementing the leaching solution.

The influence of different electrolytic conditions on the purity of aluminium hydroxyfluoride hydrate products was explored, including current density of 0.2−1.0 A/cm^2, electrolytic temperature of 50−90 °C, stirring speed of 100−500 r/min, and electrolytic end pH of 2.0−4.5.

(3) Roasting test

The aluminium hydroxyfluoride hydrate precipitations obtained in Step (2) were mixed to roast to prepare anhydrous aluminum fluoride.

To inhibit the hydrolysis of aluminium hydroxyfluoride hydrate at high temperature, ammonium hydrogen difluoride was added before roasting. Under the condition of a roasting temperature of 550 °C and roasting time of 2 h, the influence of the mass ratio of aluminium hydroxyfluoride hydrate to ammonium hydrogen difluoride on the purity of aluminum fluoride products was investigated to determine the optimal ratio of roasting ingredients.

2.3.2 Analysis and characterization

(1) The phase composition structure of a solid phase sample is determined by using the X-ray diffractometer (XRD) type of PANalytical/Reying 2Empyrean 2 (PANalytical B. V., Netherlands). The powder sample was prepared by the tablet crushing method.

(2) The micromorphology of solid-phase samples was characterized by the field emission scanning electron microscope (SEM) type of the MIRA4 LMH (TESCAN, a. s. in Brno, Czech Republic).

(3) The liquid phase composition was quantitatively analyzed by using the external standard method via an inductively coupled plasma emission spectrometer (ICP) type of the iCAP 7400 Radial (Thermo Fisher Scientific, USA).

(4) According to the national standard determination method GB/T 34500.1—2017, the fluorine ion selective electrode method was used to quantitatively analyze the fluorine ion concentration in the liquid phase. The instrument selected a PXSJ−226 ion meter, PF-2-01 fluoride ion electrode, and 232 reference electrode (Shanghai REX Instrument Co., Ltd.).

The formula for the leaching rate of fluoride (E_F) is as follows:

$$E_F=\frac{c_F\cdot V\cdot M_F}{w_F\cdot m_w} \tag{5}$$

where c_F is the molar concentration of F in the leaching solution (mol/L), V is the volume of the leaching solution (L), M_F is the relative atomic mass of F, and w_F is the content of F in waste aluminum electrolyte.

3 Results and discussion

3.1 Effect of leaching conditions on leaching rate of fluoride ions

The effect of different leaching conditions on the leaching rate of fluoride ions is shown in Fig. 5. Under the leaching temperature of 90 °C and leaching time of 2 h, the effects of the L/S ratio and F/Al ratio were studied. As illustrated in Fig. 5(a), when the F/Al ratio is kept constant, the leaching rate of fluorine ions is effectively improved overall with the increase of the L/S ratio from 8 to 12. For example, when F/Al ratio is 2.0, the leaching rate of fluoride ions with L/S ratio of 12 increases by 3.9% compared with L/S ratio of 8. This is because the increase in the L/S ratio is beneficial to reduce the slurry viscosity and increase the diffusion rate of aluminum chloride solvent, thus accelerating the leaching reaction. At the same time, according to the chemical equilibrium, the increase of L/S ratio is conducive to the balance to move to the leaching direction, thereby improving the leaching rate of fluoride ions.

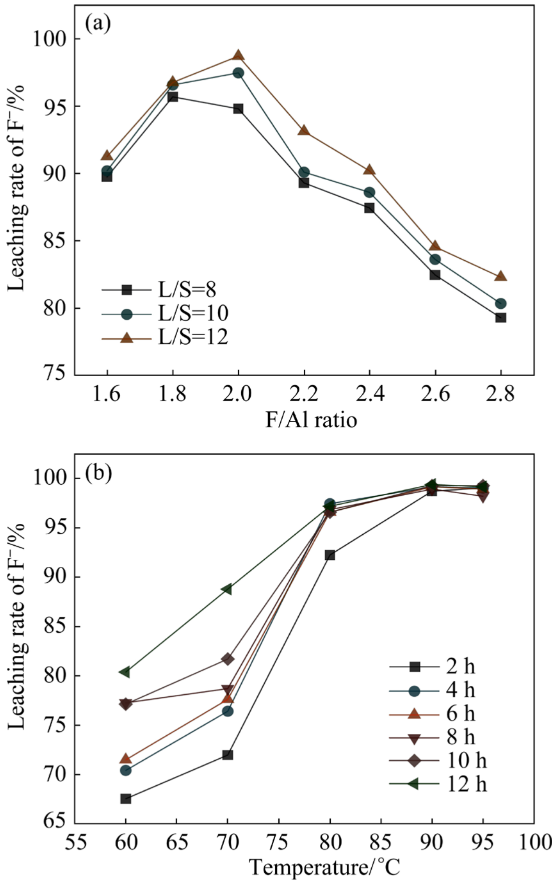

Fig. 5 Effects of different conditions on leaching rate of F⁻: (a) L/S ratio (T=90 °C, t=2 h); (b) Leaching time (F/Al ratio=2.0, L/S=12)

Under the unchanged condition of L/S ratio, when the F/Al ratio increased from 1.6 to 2.8, the leaching rate of fluoride ions overall showed a trend of rising first and then decreasing. For example, when L/S ratio is 12, with the increase of F/Al ratio, the leaching rate of fluoride ion will keep growing until F/Al ratio is 2.0, when the leaching rate reaches the maximum of 98.65%, which increased by 7.41% compared with F/Al ratio of 1.6. From then on, keeping the F/Al ratio improved resulted in the leaching rate decreasing. When F/Al ratio is 2.8, the leaching rate is only 82.28%. According to the analysis, it can be seen that the increase of F/Al ratio to a certain extent is conducive to the preferential combination of aluminum ions and fluorine ions to form a complex, which consumes the free fluorine ions in the solution, thus promoting the dissociation of fluorine in the solid phase and improving the leaching rate of fluorine ions. However, when F/Al ratio exceeds a certain limit, in other words, when Al^{3+} is too small, the content of Al^{3+} is not enough to consume fluorine ions in the solution, which will result in the reduction of the number of aluminum fluorine complex groups formed with fluorine reduced, as a consequence of reducing the complexation efficiency and the leaching rate of fluorine ions. The higher the F/Al ratio is, the lower the fluorine ion leaching rate will be.

At F/Al ratio of 2.0 and L/S ratio of 12, the effects of the leaching temperature and leaching time were studied. As can be seen from Fig. 5(b), raising the leaching temperature is more effective in improving the leaching rate of fluoride ions than extending the leaching time. At 60 and 70 °C, the leaching rate can be increased by 1% to 7% every 2 h. But when the temperature rises to 80−95 °C, the extension of leaching time has no obvious effect on the improvement of fluoride ion leaching rate. When the leaching time was unchanged, with the temperature ranging from 60 to 80 °C, the fluorine ion leaching rate increased significantly. When the leaching time was 4 h, the fluorine ion leaching rate increased from 70.40% at 60 °C to 97.43% at 80 °C. With further rising in the temperature, the fluorine ion leaching rate increased slightly, but the change was not significant. This is because the increase in temperature improves the solubility of some soluble components in the solid phase under the same leaching time conditions. Meanwhile, it is conducive to increasing the diffusion speed, and thus promoting the fluoride ions leaching rate. However, when the temperature rises to a certain extent, the complexation of aluminum and fluoride ions is close to the limit, which slows down the effect of high temperature. The leaching rate reached 99.15% when the leaching temperature was 90 °C and the leaching time was 4 h.

According to the experimental results, the optimal conditions for the leaching experiment were as follows: F/Al=2.0, L/S=12, leaching temperature 90 °C, and leaching time 4 h.

3.2 Effect of electrolytic conditions on purity of aluminium hydroxyfluoride hydrate

Figure 6 shows the effect of different electrolytic conditions on the purity of aluminium hydroxyfluoride hydrate. The changing trend of total impurity content in aluminium hydroxyfluoride hydrate is consistent with that of Na and K impurities. But the content of Ca does not fluctuate significantly with the change of current density, temperature, stirring speed, and electrolytic endpoint pH. The Ca content is relatively low, ranging from 0.11 to 0.16 wt.%.

Setting the stirring speed to 200 r/min, the electrolytic temperature at 80 °C, and the electrolytic endpoint of leaching solution pH under 2.5, the effect of the current density on the impurity content of precipitation was investigated, and the results are shown in Fig. 6(a). With the current density increasing from 0.2 to 1.0 A/cm^2, the contents of Na and K impurities in aluminium hydroxyfluoride hydrate continue to increase, and the lowest content is found at 0.2 A/cm^2. When the current density is greater than 0.6 A/cm^2, the impurity content of Na and K exceeds 1%. When the current density is 1.0 A/cm^2, the Na content is as high as 2.03 wt.%. This is because the increase in current density accelerates the migration rate of the Al−F complex ion and the combination rate with hydroxide ion. This results in the faster formation rate of aluminium hydroxyfluoride hydrate crystal nucleus and smaller grain size, which makes the sediment layer easy to include impurity elements. On the other hand, according to Faraday’s first law and Ohm’s law, the amount of reduction products precipitated on the cathode is proportional to the current density. The polarization effect is more visible as the current density increases. Then, the reaction rate of hydrogen ion reduction to hydrogen gas and the separation rate of hydroxide ions would be accelerated. Finally, it will increase the alkalinity near the cathode and promote the precipitation of cryolite impurities. When the current density is 0.2 A/cm^2, the contents of Na, K and Ca in aluminium hydroxyfluoride hydrate products are0.57, 0.24 and 0.13 wt.% respectively, and the total impurity contents are 0.94 wt.%.

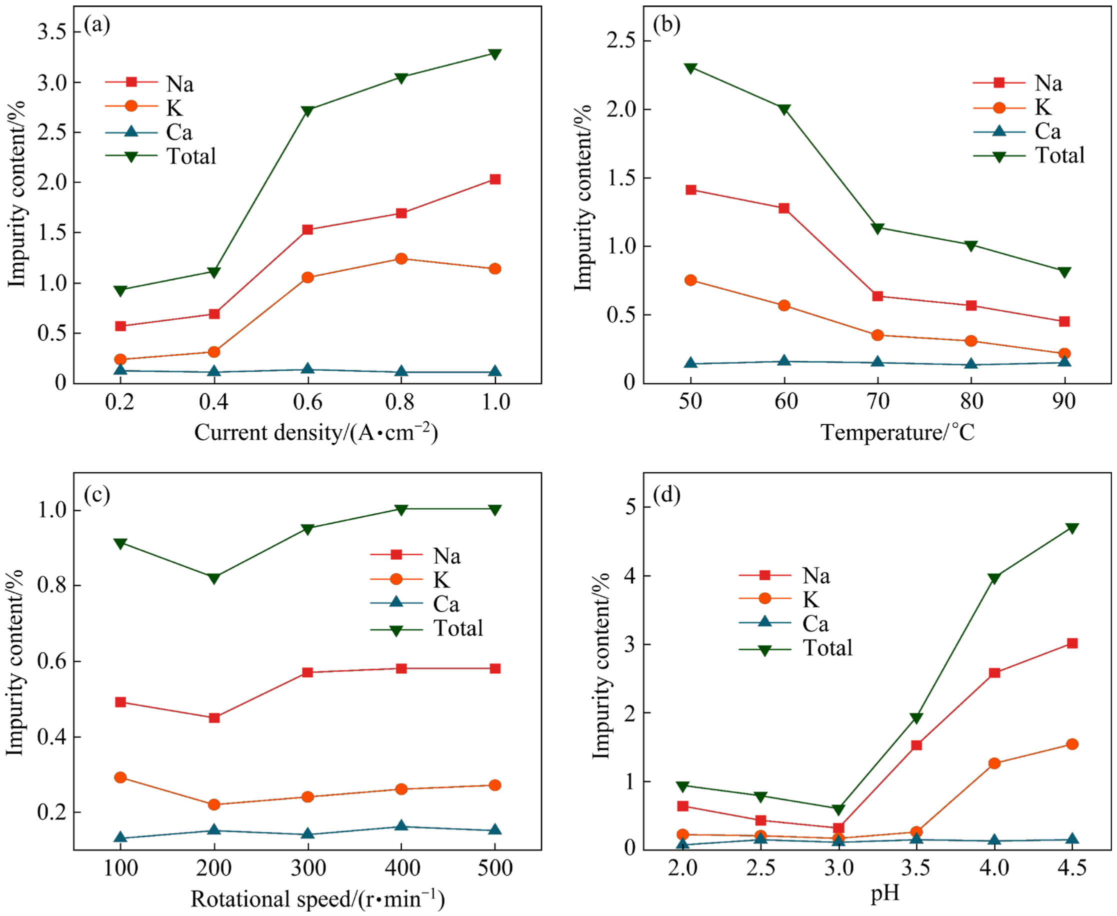

Fig. 6 Effect of different electrolytic conditions on impurity content of aluminium hydroxyfluoride hydrate products: (a) Current density; (b) Temperature; (c) Rotational speed; (d) Electrolytic endpoint pH

The electrolytic temperature also has an obvious influence on the impurity content of the product. The experimental results are shown in Fig. 6(b) at a controlled current density of 0.2 A/cm^2, stirring speed of 200 r/min, and electrolytic end pH of 2.5.

When the electrolytic temperature is 50 °C, the total impurity concentration in aluminium hydroxyfluoride hydrate is 2.35 wt.%. With the electrolytic temperature gradually rising to 90 °C, the contents of Na and K impurities continue to decrease. When the electrolytic temperature is 90 °C, the Na and K contents are reduced by 0.96% and 0.54%, respectively compared with those at 50 °C. This is because the solubility of aluminium hydroxyfluoride hydrate decreases with increasing temperature [35], while the solubility of cryolite increases [36]. High temperature is more favorable for AlF^{2+} and AlF_2^+ complex ion groups to combine with the hydroxide to precipitate aluminium hydroxyfluoride hydrate, reducing the precipitation of cryolite with Na and K impurities. When the electrolytic temperature is 90 °C, the total impurities in aluminium hydroxyfluoride hydrate are the lowest (0.82 wt.%), and the contents of Na, K and Ca impurities are 0.45, 0.22 and 0.15 wt.% respectively. Considering that continuing to increase the temperature has little effect on the impurity content, the electrolytic temperature is finally chosen to be 90 °C.

Under the conditions of the current density of 0.2 A/cm^2, the electrolytic temperature of 90 °C, and the pH 2.5 of the electrolytic endpoint, the influence of stirring speed on the purity of precipitated aluminium hydroxyfluoride hydrate was investigated and the results are shown in Fig. 6(c). In the figure, when the stirring speed is gradually increased from 100 to 500 r/min, the impurity contents of Na and K in aluminium hydroxyfluoride hydrate show a trend of decreasing first and then increasing. When the stirring speed is faster than 300 r/min, the increasing trend of Na and K slows down, and the change is not obvious. Because increasing the stirring speed within a certain range will speed up the transmission rate of ions in solution and increase the opportunity for hydroxide ions to full contact with Al−F complex ions, which precipitates the aluminium hydroxyfluoride hydrate more uniformly and stably and reduces the precipitation of a small amount of cryolite due to the high concentration of hydroxide ions in local areas. Therefore, the content of Na and K impurities in aluminium hydroxyfluoride hydrate is reduced. However, when the stirring speed is too fast, the formation rate of aluminium hydroxyfluoride hydrate crystal nucleus is higher than the growth rate. In addition, the rapid stirring speed will also destroy the formed crystal nucleus and result in fine-grained products, which can easily cause impurity inclusion and increase the content of Na and K. When the stirring speed was 200 r/min, the total impurity concentration was the lowest (0.82 wt.%).

In addition to the above factors, the choice of the electrolysis end node is also very important. Therefore, under the conditions of current density of 0.2 A/cm^2, electrolytic temperature of 90 °C, and stirring speed of 200 r/min, the effects of electrolytic endpoint pH in the range of 2.0−4.5 on impurity content were studied, and the results are shown in Fig. 6(d). When the endpoint pH of the solution was less than 3.0, the K content showed no significant change and remained at about 0.2 wt.%, and the Na content slowly decreased as the pH increased. The electrolysis ends at a low pH, which means that the electrolysis time is short. The aluminium hydroxyfluoride hydrate has just begun to form at this time, resulting in the degree of crystallization being weak and the particle size being small. The precipitation in colloidal form is easy to intermingle and adhere to other impurities, thus reducing the purity of aluminium hydroxyfluoride hydrate. When the pH is higher than 3.0, the content of Na and K impurities increases significantly. The total impurity content reached 4.75 wt.% at pH 4.5, which was 4.1% higher than that at pH 3.0. This is because, as the electrolytic process proceeds, the release of hydrogen gas results in a gradual increase in the pH of the solution. Therefore, the aluminum and fluorine in the solution tend to form highly coordinated complex groups, and then combine with Na and K ions to form cryolite impurities. At pH 3.0, the contents of Na, K and Ca in aluminum hydroxyl fluoride were respectively 0.33, 0.18 and 0.13 wt.%, and the total content is 0.64 wt.%.

Medusa software [37] was used to simulate the distribution of different complex ions of aluminum and fluorine in solution as a function of pH, as shown in Fig. 7. The data of the Chemical Equilibrium Constant were taken from the references [25,34]. It can be seen from the figure that F^- and Al^{3+} exist stably in solution in the form of AlF^{2+} and AlF_2^+ at low pH. However, with the increase of pH, AlF^{2+} and AlF_2^+ gradually transform into AlF_4^-, AlF_5^{2-} and AlF_6^{3-} complex groups, which will easily combine with Na^+ in solution to form cryolite. This simulation indicates that the experimental results are consistent with the variation trend of complex ions.

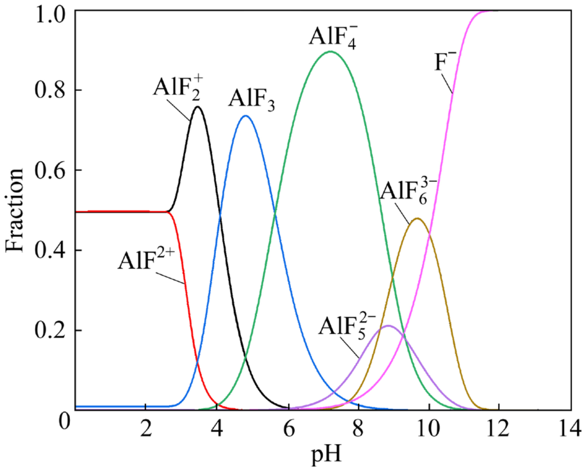

Fig. 7 Distribution of Al−F complex ions as function of pH (25 °C)

Combined with the experimental results, the optimal conditions of the electrolysis experiment are as follows: current density 0.2 A/cm^2, electrolytic temperature 90 °C, stirring speed 200 r/min, and electrolytic endpoint pH 3.0. In this case, the total impurity content of Na, K and Ca was only 0.64 wt.%.

The XRD results of aluminium hydroxyfluoride hydrate obtained from the optimal electrolytic experimental conditions and by traditionally adding lye to adjust the pH are shown in Fig. 8. After comparison and analysis, the $Na_5Al_3F_{14}$ impurity phase appeared in the product obtained by adding lye, but there is no impurity peak in the product obtained by electrolysis experiment. In addition, the diffraction peak of aluminium hydroxyfluoride hydrate by electrolysis is stronger, indicating that the crystallization degree is higher than that of the product by adding lye. Therefore, the electrolysis method is more advantageous to obtain high-purity aluminium hydroxyfluoride hydrate.

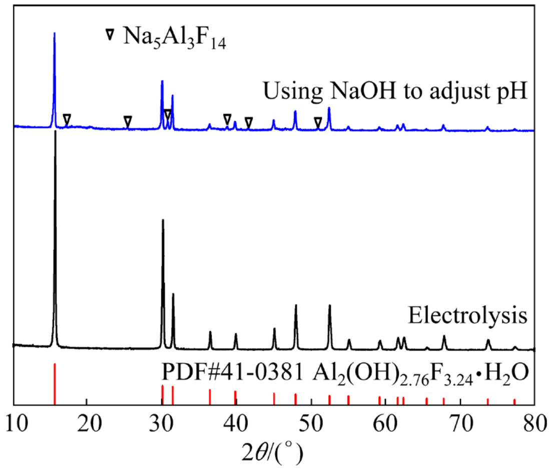

Fig. 8 XRD patterns of aluminium hydroxyfluoride hydrate

The aluminium hydroxyfluoride hydrate under optimal electrolysis conditions was analyzed by scanning electron microscopy (SEM), and the results are shown in Fig. 9. The microscopic morphology of aluminium hydroxyfluoride hydrate is irregular polygons, and its crystal grains are attached to each other to grow, whose particle sizes are 50−100 nm with a uniform distribution.

3.3 Effect of mixture ratio in roasting on aluminum fluoride products

Ammonium hydrogen fluoride (NH_4HF_2) was mixed with aluminium hydroxyfluoride hydrate for roasting, and the results are shown in Fig. 10. It can be seen that with the increase of ammonium hydrogen fluoride dosage, the purity of aluminum fluoride obtained by roasting is improved. The high ratio of aluminium hydroxyfluoride hydrate to ammonium hydrogen fluoride means a small amount of ammonium hydrogen fluoride. So it is not enough to inhibit the hydrolysis of aluminium hydroxyfluoride hydrate and supply fluorine supplements at the same time. During roasting, the partial hydrolysis of aluminium hydroxyfluoride will hydrate to generate aluminum oxide and hydrogen fluoride, thereby reducing the purity of aluminum fluoride. When the mass ratio of the mixture is 2∶1, the purity of aluminum fluoride is up to 99.51 wt.%, and the purity is unchanged by increasing the dosage of ammonium hydrogen fluoride. Therefore, the optimal ratio of aluminium hydroxyfluoride hydrate to ammonium hydrogen fluoride is 2∶1.

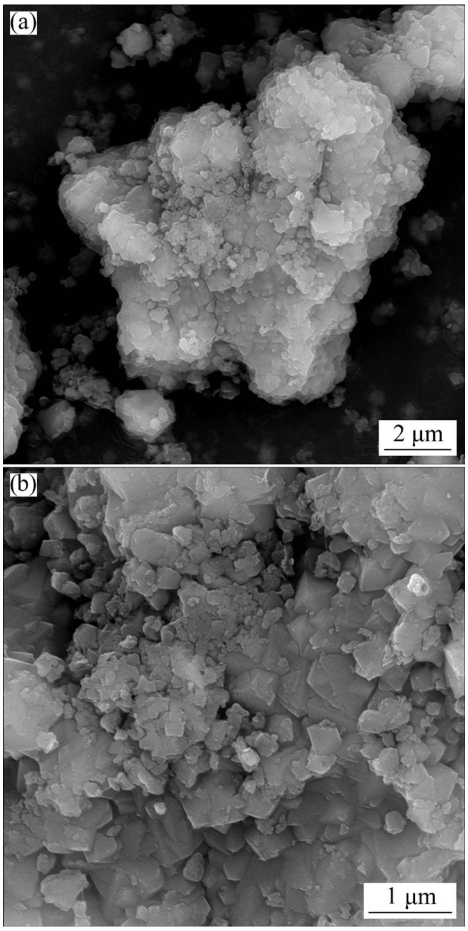

Fig. 9 SEM images of aluminum hydroxyl fluoride

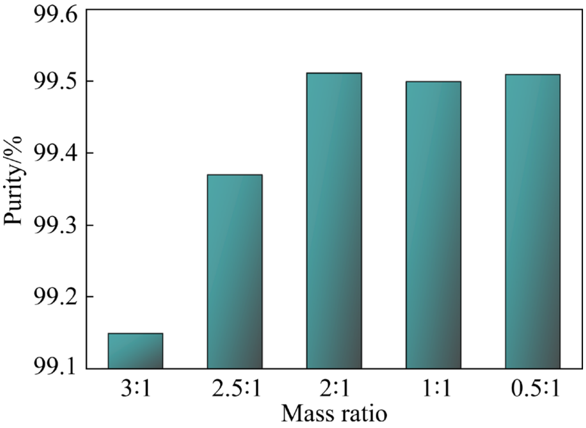

Fig. 10 Effect of mass ratio of aluminium hydroxyfluoride hydrate to ammonium hydrogen fluoride on purity of aluminum fluoride

High-purity aluminum fluoride was obtained under the experimental conditions of an optimal ratio of ingredients. The phase analysis was carried out and compared with the aluminum fluoride obtained from the direct roasting of aluminium hydroxyfluoride hydrate shown in Fig. 11. It can be seen from the figure that the phase of the product roasted with ammonium hydrogen fluoride is AlF_3 with no impurity peak appearing, while a small amount of Al_2O_3 impurity phase appears in the product obtained by direct roasting. In addition, compared with direct roasting, aluminum fluoride obtained by adding ammonium hydrogen fluoride for mixed roasting has a stronger diffraction peak and a higher crystallization degree.

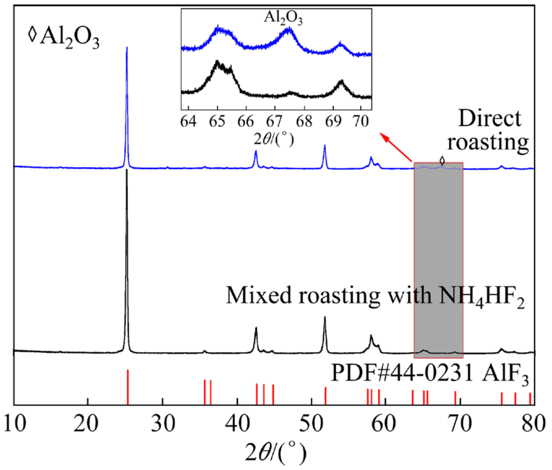

Fig. 11 XRD patterns of aluminum fluoride

The direct roasting result is consistent with Eq. (6) mentioned by LISBONA and STEEL [34]. The aluminium hydroxyfluoride hydrate decomposed into aluminum fluoride, alumina and hydrogen fluoride by direct roasting. Under the condition of high temperature, HF volatilizes, while Al_2O_3 remains in the solid phase product and mixes with AlF_3. However, the XRD analysis is not obvious because Al_2O_3 is amorphous.

$$3AlF_2(OH) \rightarrow AlF_3 + Al_2O_3 + 3HF\uparrow \tag{6}$$

In addition, because the hydroxyl aluminum fluoride contains crystal water, AlF_3 will be hydrolyzed to alumina at high temperature, which will result in fluorine loss and reduce the content of aluminum fluoride in the product. The hydrolytic reaction of AlF_3 is shown as follows [38]:

$$2AlF_3 + 3H_2O \rightarrow Al_2O_3 + 6HF\uparrow \tag{7}$$

It is speculated that the reaction formula of mixed roasting of ammonium hydrogen fluoride and aluminium hydroxyfluoride hydrate is shown in Eq. (8). The products of mixed roasting are AlF_3, NH_3, HF and H_2O. After gas-phase substances volatilize, the solid phase is only AlF_3, which effectively avoids the residue of Al_2O_3.

$$Al_2(OH)_{2.76}F_{3.24}\cdot H_2O + 2NH_4HF_2 \rightarrow 2AlF_3 + 2NH_3\uparrow + 1.24HF\uparrow + 3.76H_2O\uparrow \tag{8}$$

AlF_3 obtained by direct roasting was analyzed by X-ray photoelectron spectroscopy (type of the ESCALAB 250Xi, Thermo Fisher Scientific, USA), which further confirmed that direct roasting would cause the decomposition of hydroxyl aluminum fluoride to produce alumina. The XPS result is shown in Fig. 12, where the Al 2p peak is fitted into two symmetric single peaks, corresponding to the Al—O and Al—F bonds, which are consistent with the reported binding energies of 74.6 and 77.27 eV for γ-$A_{l2}O_3$ and α-AlF_3 [39,40].

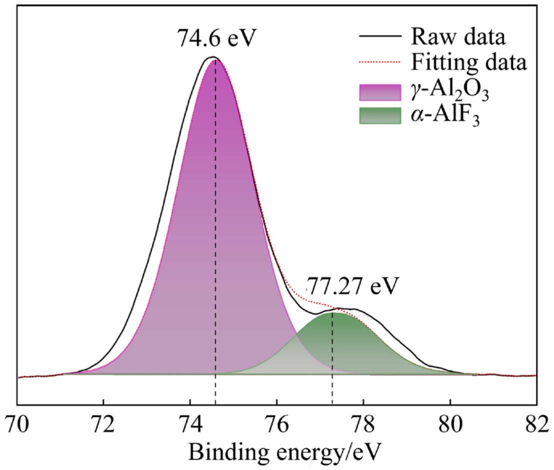

Fig. 12 XPS result of products obtained by direct roasting

The composition of aluminum fluoride was analyzed, and the results are shown in Table 2. In the aluminum fluoride products obtained in this study, the total impurity content of Na and other elements is 0.49 wt.%, which is lower than the composition requirement of the national standard GB/T 4292—2017 [41] for AF-0 anhydrous aluminum fluoride. Therefore, the aluminum fluoride can be returned directly to the aluminum electrolysis cell or used as a chemical agent.

Table 2 Element content in aluminum fluoride (wt.%)

F	Al	Na	O	Others	Method	Source
67.52	31.98	0.20	0.03	0.27	Mixed roasting with NH_4HF	This work
47.33	36.71	0.44	15.10	0.42	Direct roasting	This work (comparison)
58.80	27.90	1.25	−	−	Mixed roasting with HF	Ref. [33]
−	−	0.83	−	−	Direct roasting	Ref. [32]
−	−	2.45	−	−	Direct roasting	Ref. [34]
≥61.0	≥31.5	≤0.30	−	−	−	AF-0 (GB/T 4292—2017)
≥60.0	≥31.0	≤0.40	−	−	−	AF-1 (GB/T 4292—2017)
≥60.0	≥31.0	≤0.60	−	−	−	AF-2 (GB/T 4292—2017)

Note: The mass fraction of AlF_3 in Ref. [32] is 54.4%; the molar ratio of F to Al in Ref. [34] is 1.79

4 Conclusions

(1) A new process was proposed to extract valuable aluminum and fluoride from waste aluminum electrolytes to prepare high-purity aluminum fluoride products. There are three main steps, including aluminum chloride leaching, electrolysis leaching solution, and mixed roasting with ammonium hydrogen fluoride.

(2) In the procedure of leaching, when the F/Al ratio is 2.0, the L/S is 12, the leaching temperature is 90 °C, and the leaching time is 4h, the optimal fluoride ion leaching rate is 99.15%.

(3) The electrolysis method can effectively avoid the precipitation of cryolite impurities. Under the optimal conditions of the current density of 0.2 A/cm^2, the temperature of 90 °C, stirring speed of 200 r/min, and electrolysis end pH of 3.0, the total content of Na K, and Ca impurities in aluminium hydroxyfluoride hydrate is only 0.64 wt.%.

(4) The purity of the AlF_3 obtained by adding ammonium hydrogen fluoride for mixed roasting is higher than that obtained by direct roasting. When the ratio of aluminium hydroxyfluoride hydrate to ammonium hydrogen fluoride is 2:1, the purity of the aluminum fluoride product is 99.51 wt.%, which is higher than the composition requirements of the national standard GB/T 4292—2017 for AF-0 anhydrous aluminum fluoride.

CRediT authorship contribution statement

Xiao-jun LV: Conceptualization, Methodology, Supervision, Resources, Formal analysis, Writing − Original draft; **Xuan TAN:** Investigation, Data curation, Formal analysis, Writing − Review & editing; **Ze-xun HAN:** Project administration, Methodology, Writing − Review & editing; **Li-qiong LUO:** Validation, Writing − Review & editing; **Yong-cong WU:** Visualization, Writing − Review & editing.

Declaration of competing interest

The authors declare that they have no known competing financial interests or personal relationships that could have appeared to influence the work reported in this paper.

References

[1] DENG Xu, ZHANG Xiang-min. Current status and future development trend of secondary aluminum industry [J]. Resource Recycling, 2020(11): 27−29. (in Chinese)

[2] HAN Jian-jun. Study on recovery process of lithium-containing electrolyte produced by electrolytic aluminum industry [J]. Henan Chemical Industry, 2018, 35(10): 24−27. (in Chinese)

[3] TAO Wen-ju, YANG Jia-xin, CHEN Li-yu, ZHANG Yi-fan, WU Shao-hua, LI Jia-ming, LIU Zhao-shun, HE Jin-gui, WANG Zhao-wen. Sustainable recovery of fluorine from waste aluminum electrolyte by sulfuric acid baking [J]. Journal of Sustainable Metallurgy, 2023, 9(3): 1201−1214.

[4] HOLYWELL G, BREAULT R. An overview of useful methods to treat, recover, or recycle spent potlining [J]. JOM, 2013, 65(11): 1441−1451.

[5] XIE Ming-zhuang, LI Rong-bin, ZHAO Hong-liang, LIU Wei, LU Ting-ting, LIU Feng-qin. Detoxification of spent cathode carbon blocks from aluminum smelters by joint controlling temperature-vacuum process [J]. Journal of Cleaner Production, 2020, 249: 119370.

[6] ZHAO Hong-liang, MA Bao-zhong, HONG Shuang, HUANG Hao, LIU Feng-qin, SOHN H Y. Recovery of copper and cobalt from converter slags via reduction-sulfurization smelting using spent pot lining as the reductant [J]. ACS Sustainable Chemistry & Engineering, 2021, 9(11): 4234−4246.

[7] ANDRADE-VIEIRA L F, TRENTO M V C, CÉSAR P H S, MARCUSSI S. Spent pot liner from aluminum industry:

Genotoxic and mutagenic action on human leukocytes [J]. Environmental Science and Pollution Research, 2019, 26(27): 27640−27646.

[8] National Bureau of Statistics. Statistical Bulletin of the People's Republic of China on National Economic and Social Development in 2022 [EB/OL]. 2023-11-13. https://www.gov.cn/xinwen/2023-02/28/content_5743623.htm (in Chinese)

[9] WANG Dong-yue, WANG Hai-bin, LI Chun-lei, QI Yong-rong, FAN Li-ting, PENG Li. Process for stabilizing fluorine in electrolytic aluminum spent pot lining by roasting method [J]. IOP Conference Series: Earth and Environmental Science, 2021, 621(1): 012036.

[10] LI Rong-bin, LU Ting-ting, XIE Ming-zhuang, LIU Feng-qin. Analysis on thermal behavior of fluorides and cyanides for heat-treating spent cathode carbon blocks from aluminum smelters by TG/DSC-MS & ECSA® [J]. Ecotoxicology and Environmental Safety, 2020, 189: 110015.

[11] XIN Xin, ZHAO Jun-xue, HU Ai-lin, WANG Ze, KANG Yi, REN Meng-meng, LI Bin, TANG Wen-dan. High-temperature vacuum treatment of aluminum electrolytic spent carbon cathode [J]. Journal of Sustainable Metallurgy, 2022, 8(3): 1204−1214.

[12] NUNEZ P. Developing guidance to support sustainable spent pot lining (SPL) management across the aluminum industry [J]. JOM, 2020, 72(10): 3334−3340.

[13] LI Yi-fan, CHENG Hao, GONG Pei-yu, YANG Kai, TIAN Zhong-liang, LAI Yan-qing. An environmentally benign and sustainable process for carbon recovery and efficient defluorination of spent carbon cathode [J]. Transactions of Nonferrous Metals Society of China, 2022, 32(11): 3810−3821.

[14] XU Rui, LUO Sha, LI Wen-zhang, ZHANG Chen-yu, CHEN Zi-hao, WANG Yue, LIU Yang, LI Jie. Clean process for selective recovery of lithium carbonate from waste lithium-bearing aluminum electrolyte slag [J]. Industrial & Engineering Chemistry Research, 2023, 62(36): 14537−14547.

[15] WU Shao-hua, TAO Wen-ju, GE Hui, YANG Jia-xin, CHEN Li-yu, HE Jin-gui, YANG You-jian, WANG Zhao-wen. Extraction and recycling of fluoride-containing phase from spent bottom sedimentation of aluminum smelting cell by leaching in Al^{3+} solution media [J]. Separation and Purification Technology, 2023, 306: 122797.

[16] YUAN Ya, YU Xiao-hua, SHEN Qing-feng, ZHAO Qun, LI Yong-gang, WU Ting. A novel approach for ultrasonic assisted organic acid leaching of waste lithium-containing aluminum electrolyte and recovery of lithium [J]. Chemical Engineering and Processing: Process Intensification, 2023, 192: 109508.

[17] SUN Guang, ZHANG Gang, LIU Jing-yong, XIE Wu-ming, EVRENDILEK F, BUYUKADA M. (Co-)combustion behaviors and products of spent potlining and textile dyeing sludge [J]. Journal of Cleaner Production, 2019, 224: 384−395.

[18] CHEN Yu-ran, LI Pan, BU Xiang-ning, CHEHREH-CHELGANI S, KONG Ya-peng, LIANG Xue-min. Resource utilization strategies for spent pot lining: A review of the current state [J]. Separation and Purification Technology, 2022, 300: 121816.

[19] WANG Yao-wu, PENG Jian-ping, DI Yue-zhong. Separation and recycling of spent carbon cathode blocks in the aluminum industry by the vacuum distillation process [J]. JOM, 2018, 70(9): 1877−1882.

[20] YAO Zhen, ZHONG Qi-fan, XIAO Jin, YE Sheng-chao, TANG Lei, ZHANG Zhen-hua. An environmental-friendly process for dissociating toxic substances and recovering valuable components from spent carbon cathode [J]. Journal of Hazardous Materials, 2021, 404: 124120.

[21] CORRAL-CAPULIN N G, VILCHIS-NESTOR A R, GUTIÉRREZ-SEGURA E, SOLACHE-RÍOS M. The influence of chemical and thermal treatments on the fluoride removal from water by three mineral structures and their characterization [J]. Journal of Fluorine Chemistry, 2018, 213: 42−50.

[22] TANG Chao-bo, WANG Jia-hui, YANG Sheng-hai, ZHANG Xian-pan, LI Shuai, LAI Yan-qing, TIAN Zhong-liang, JIN Sheng-ming, CHEN Yong-ming. Efficient extraction and recovery of lithium from waste aluminum cryolite electrolyte [J]. Resources, Conservation & Recycling, 2023, 197: 107070.

[23] WU Shao-hua, TAO Wen-ju, ZHENG Yan-chen, YANG You-jian, YU Jiang-yu, CUI Jing-bo, LU Yu, SHI Zhong-ning, WANG Zhao-wen. Novel process for the extraction of lithium carbonate from spent lithium-containing aluminum electrolytes by leaching with aluminum nitrate and nitric acid [J]. Hydrometallurgy, 2020, 198: 105505.

[24] HAN Ze-xun, WU Yong-chong, HAO Peng-cheng, TAN Xuan, WEI Ming-ren, LV Xiao-jun. Efficient lithium recovery from lithium-containing spent aluminium electrolyte via NaF fluorination roasting and $Al_2(SO_4)_3$ leaching [J]. Journal of Environmental Chemical Engineering, 2023, 11(5): 110948.

[25] HAN Ze-xun, LUO Li-qiong, WU Yong-cong, HAO Peng-cheng, TAN Xuan, LV Xiao-jun. Cryolite-induced crystallization defluorination process of spent aluminium electrolyte leaching solution [J]. Journal of Central South University (Science and Technology), 2023, 54(2): 595−600. (in Chinese)

[26] CAO Xiao-zhou, SHI Yuan-yuan, ZHAO Shuang, XUE Xiang-xin. Recovery of valuable components from spent pot-lining of aluminium electrolytic reduction cells [J]. Journal of Northeastern University (Natural Science), 2014, 35(12): 1746−1749. (in Chinese)

[27] WU Shao-hua, TAO Wen-ju, ZHENG Yan-chen, GE Hui, HE Jin-gui, YANG You-jian, WANG Zhao-wen. A novel approach for lithium recovery from waste lithium-containing aluminum electrolyte by a roasting-leaching process [J]. Waste Management, 2021, 134: 89−99.

[28] BARANOV A N, GAVRILENKO A A, VOLYANSKII V V, GAVRILENKO L V, NOZHKO S I, TIMKINA E V. Technology for preparing calcium fluoride from aluminum production waste [J]. Metallurgist, 2017, 61(5/6): 485−490.

[29] DAVID H J. Recovery of aluminium and fluoride values from spent pot lining: America, US05352419(A) [P]. 1994−10−04.

[30] LISBONA D F, SOMERFIELD C, STEEL K M. Leaching of spent pot-lining with aluminium nitrate and nitric acid: Effect of reaction conditions and thermodynamic modelling

of solution speciation [J]. Hydrometallurgy, 2013, 134/135: 132−143.

[31] NIE Yun-fei, GUO Xin-yao, GUO Zhao-hui, TANG Jian-guo, XIAO Xi-yuan, XIN Li-qing. Defluorination of spent pot lining from aluminum electrolysis using acidic iron-containing solution [J]. Hydrometallurgy, 2020, 194: 105319.

[32] BUSH J F, GAYDOSIK G F. Aluminum-fluorine compound manufacture: Canada, CA1210565(A) [P]. 1986−09−02.

[33] WU Shao-hua, TAO Wen-ju, HAN Wang, GE Hui, CHEN Li-yu, YANG Jia-xin, ZHENG Yan-chen, HE Jin-gui, YANG You-jian, WANG Zhao-wen. Hydrometallurgical stepwise separation of alumina and recovery of aluminum fluoride from waste anode cover material of aluminum electrolysis [J]. Minerals Engineering, 2022, 186: 107740.

[34] LISBONA D F, STEEL K M A. Recovery of fluoride values from spent pot-lining: Precipitation of an aluminium hydroxyfluoride hydrate product [J]. Separation and Purification Technology, 2008, 61(2): 182−192.

[35] NTUK U, TAIT S, WHITE E T, STEEL K M. The precipitation and solubility of aluminium hydroxyfluoride hydrate between 30 and 70 °C [J]. Hydrometallurgy, 2015, 155: 79−87.

[36] AIGUEPERSE J, MOLLARD P, DEVILLIERS D, CHEMLA M, FARON R, ROMANO R, CUER J P. Fluorine compounds, inorganic [M]//Encyclopedia of Industrial Chemistry. France: Fritz Ullmann, 2000: 414−415.

[37] PUIGDOMÈNECH I, COLÀS E, GRIVÉM, CAMPOS I, GARCÍA D. A tool to draw chemical equilibrium diagrams using SIT: Applications to geochemical systems and radionuclide solubility [J]. MRS Online Proceedings Library, 2014, 1665(1): 111−116.

[38] YAN Heng-wei, KUANG Ye, YANG Yong-hui, GAO Ji-yan, LIU Zhan-wei. Preparation of anhydrous aluminum fluoride [J]. Results in Chemistry, 2023, 100919.

[39] STROHMEIER B R. Gamma-alumina (γ-Al_2O_3) by XPS [J]. Surface Science Spectra, 1994, 3(2): 135−140.

[40] BÖSE O, KEMNITZ E, LIPPITZ A, UNGER W E S. α-AlF_3 by XPS and XAES referenced by Au 4f7/2 [J]. Surface Science Spectra, 1998, 5(1): 75−81.

[41] GB/T 4292—2017, Aluminium fluoride [S]. (in Chinese)

采用浸出、电解和焙烧工艺从废铝电解质中制备 AlF_3

吕晓军，谭 璇，韩泽勋，罗丽琼，吴勇聪

中南大学 冶金与环境学院，长沙 410083

摘 要：以废铝电解质为原料，采用氯化铝浸出、电解浸出液和氟化氢铵混合焙烧相结合的工艺制备高纯 AlF_3。在氟铝摩尔比为 2.0、液固比为 12、温度为 90 ℃及时间为 4 h 的最佳浸出条件下，氟的浸出率可达到 99.15%。在电解作用下，阴极的 H^+被还原成 H_2，余下的 OH^-与 AlF_2^+和 AlF^{2+}结合，形成羟基氟化铝沉淀物。结果表明，电解有利于降低羟基氟化铝的杂质含量，当电流密度为 0.2 A/cm^2、温度为 90 ℃、搅拌速度为 200 r/min、电解终点 pH 为 3.0 时，沉淀中的 Na、K 和 Ca 杂质总含量仅为 0.64%(质量分数)。此外，添加氟化氢铵混合焙烧可有效抑制水解，当羟基氟化铝与氟化氢铵的质量比为 2∶1 时，氟化铝产品的纯度为 99.51%(质量分数)。因此，该产品可返回到铝电解工业中使用或用作试剂。

关键词：废铝电解质；氯化铝溶液；电解；羟基氟化铝；氟化氢铵；无水氟化铝

(Edited by Xiang-qun LI)